The endoplasmic reticulum-associated mRNA-binding proteins ERBP1 and ERBP2 interact in bloodstream-form *Trypanosoma brucei*

Kathrin Bajak [1,2] , **Kevin Leiss** [1] , **Christine Clayton** [1] , **Esteban Erben** [Corresp. 2]

[1] Zentrum für Molekulare Biologie der Universität Heidelberg (ZMBH), Heidelberg, Germany

[2] Deutsches Krebsforschungszentrum (DKFZ), Heidelberg, Germany

Corresponding Author: Esteban Erben
Email address: e.erben@dkfz-heidelberg.de

Kinetoplastids rely heavily on post-transcriptional mechanisms for control of gene expression, and on RNA-binding proteins that regulate mRNA splicing, translation and decay. *Trypanosoma brucei* ERBP1 (Tb927.10.14150) and ERBP2 (Tb927.9.9550) were previously identified as mRNA binding proteins that lack canonical RNA-binding domains. We here show that ERBP1 is associated with the endoplasmic reticulum, like ERBP2, and that the two proteins interact *in vivo*. Loss of ERBP1 from bloodstream-form *T. brucei* initially resulted in a growth defect but proliferation was restored after more prolonged cultivation. Pull-down analysis of tagged ERBP1 suggest that it preferentially binds to ribosomal protein mRNAs. The ERBP1 sequence resembles that of *Saccharomyces cerevisiae* Bfr1, which also localises to the endoplasmic reticulum and binds to ribosomal protein mRNAs. However, unlike Bfr1, ERBP1 does not bind to mRNAs encoding secreted proteins, and it is also not recruited to stress granules after starvation.

1 **The endoplasmic reticulum-associated mRNA-binding proteins ERBP1 and ERBP2**
2 **interact in bloodstream-form *Trypanosoma brucei*.**

3 Kathrin Bajak[a,b], Kevin Leiss[a], Christine Clayton[a] and *Esteban Erben[b]
4
5 [a]Zentrum für Molekulare Biologie der Universität Heidelberg (ZMBH), Heidelberg, Germany.
6 [b]Deutsches Krebsforschungszentrum (DKFZ), Heidelberg, Germany.
7
8 * Corresponding author: e.erben@dkfz-heidelberg.de

9 **Abstract**

10 Kinetoplastids rely heavily on post-transcriptional mechanisms for control of gene expression, and
11 on RNA-binding proteins that regulate mRNA splicing, translation and decay. *Trypanosoma brucei*
12 ERBP1 (Tb927.10.14150) and ERBP2 (Tb927.9.9550) were previously identified as mRNA
13 binding proteins that lack canonical RNA-binding domains. We here show that ERBP1 is
14 associated with the endoplasmic reticulum, like ERBP2, and that the two proteins interact *in vivo*.
15 Loss of ERBP1 from bloodstream-form *T. brucei* initially resulted in a growth defect but
16 proliferation was restored after more prolonged cultivation. Pull-down analysis of tagged ERBP1
17 suggests that it preferentially binds to ribosomal protein mRNAs. The ERBP1 sequence
18 resembles that of *Saccharomyces cerevisiae* Bfr1, which also localizes to the endoplasmic
19 reticulum and binds to ribosomal protein mRNAs. However, unlike Bfr1, ERBP1 does not bind to
20 mRNAs encoding secreted proteins, and it is also not recruited to stress granules after starvation.

21 **Introduction**
22 In *Trypanosoma brucei*, most regulation of gene expression is post-transcriptional. Protein-coding
23 genes are arranged in polycistronic transcription units, and mRNAs are excised by *trans* splicing
24 and polyadenylation (Clayton 2019). Levels of constitutively expressed proteins and mRNAs are
25 strongly influenced by codon usage (de Freitas Nascimento et al. 2018; Jeacock et al. 2018),
26 while regulation during development, over the cell cycle, and in response to environmental
27 conditions is effected mainly by RNA-binding proteins. The latter often, but not always, bind
28 sequences in 3'-untranslated regions (3'-UTRs) (Clayton 2019). All mRNAs - whether or not they
29 are subject to specific regulation - are expected to be bound by numerous different proteins,
30 forming a "messenger ribonucleoprotein" (mRNP) assembly.
31 *T. brucei* proliferates in mammalian blood and tissue fluids, and in the digestive system of Tsetse
32 flies. The developmental stages that are most accessible to laboratory study are the bloodstream
33 form, which grows at 37°C in glucose-rich media and corresponds to the form that grows in
34 mammals, and the procyclic form, which is grown at 27°C in proline-rich medium and multiplies
35 in the Tsetse midgut. Purification of mRNPs from bloodstream forms revealed at least 155
36 proteins that reproducibly could be cross-linked to, and co-purified with, mRNA (Lueong et al.
37 2016). Although many of the mRNA-binding proteins had recognizable consensus RNA-binding
38 motifs, the list included 49 proteins, including that encoded by Tb927.10.14150, which had no
39 obvious connection to RNA metabolism. Similar studies of Opisthokonts also revealed numerous
40 novel proteins without known RNA-binding domains, which have been named "enigmRBPs"

41   (Beckmann et al. 2015; Hentze et al. 2018). We will, therefore, call the Tb927.10.14150 protein
42   ERBP1 (for EnigmRBP1).
43   To assess the ability of trypanosome proteins to affect mRNA stability or translation, they were
44   "tethered" to a reporter RNA. To do this, proteins or protein fragments were expressed fused to
45   the N peptide from bacteriophage lambda. The lambdaN peptide binds an RNA stem-loop called
46   boxB with high affinity. The reporter mRNA encoded a selectable marker with boxB sequences in
47   the 3'-UTR. Proteins were screened first as random fragments (Erben et al. 2014), then at full
48   length (Lueong et al. 2016). Numerous regulators were found, many of which were also in the
49   mRNP proteome (Lueong et al. 2016), and ERBP1 reproducibly conferred a selective advantage
50   when tethered both as fragments and at full length (Erben et al. 2014; Lueong et al. 2016). ERBP1
51   fused C-terminally to GFP was associated with the endoplasmic reticulum in a high-throughput
52   screen of procyclic forms (Dean et al. 2016) and its depletion resulted in a selective disadvantage
53   in a high throughput RNAi screen (Alsford et al. 2005).
54   In this paper, we describe more detailed studies of ERBP1. ERBP1 is predicted to belong to a
55   protein family that is named after a *S. cerevisiae* protein called Bfr1p (IPR039604 or PTHR31027),
56   with alignment over its entire length. Bfr1p was originally recovered in a screen for high-copy-
57   number suppression of Brefeldin A toxicity (Jackson & Kepes 1994). It is an mRNA-binding protein
58   that is associated with polysomes and the endoplasmic reticulum (ER) (Lang et al. 2001; Weidner
59   et al. 2014), and is incorporated into stress granules (Simpson et al. 2014). In yeast, it is
60   associated with over 1000 different mRNAs, enriched for those encoding ribosomal proteins and
61   mRNAs that are translated at the ER (Lapointe et al. 2015). In addition to a role in stress granules,
62   Bfr1 has been implicated in ER quality control (Low et al. 2014) and correct nuclear segregation
63   (Xue   et   al.   1996).   The   physical   interaction   map
64   (https://www.yeastgenome.org/locus/S000005724/interaction) includes five proteins related to
65   mRNA decay: with Xrn1p, Dcp2p, Scp160p, Puf3p, and Asc1p (an orthologue of RACK1 that
66   inhibits translation). Our results reveal that ERBP1 has both similarities with, and differences from,
67   Bfr1.
68
69   **Materials and Methods**
70   **DNA manipulation and trypanosomes**
71   Lister 427 strain trypanosomes expressing the tet repressor were used for all experiments, and
72   were cultivated and transfected as described previously (Alibu et al. 2004). All plasmids and
73   oligonucleotides are listed in S3 Table. Expression from tetracycline-inducible promoters was
74   induced with 100 ng/ml tetracycline, and all growth studies were performed in the absence of
75   selecting antibiotics. Cultures that were used for RNA and protein analysis had a maximum
76   density of 1.5×10^6/ml.
77   **Western blotting**
78    $3\text{-}5 \times 10^6$ cells were collected per sample, resuspended in 6x Laemmli Buffer and heated at 95°C
79   for 10 min. The samples were subjected to SDS-PAGE gel electrophoresis using 10%
80   polyacrylamide gels. The gels were then stained with SERVA blue G or blotted on a 0.45 µm
81   nitrocellulose blotting membrane (Neolabs). To verify the protein transfer, the membrane was
82   stained with Ponceau S (SERVA). The membrane was blocked with 5% milk in TBS-Tween and
83   incubated with appropriate concentrations of first and secondary antibodies. Western Lightning
84   Ultra (Perkin Elmer) was used as a chemiluminescence system and signals were detected with

85   the LAS-4000 imager (GE Healthcare) and CCD camera (Fujifilm). Antibodies used were: rabbit
86   anti-Aldolase (1:50000) (Clayton 1987); mouse anti-myc 9E10 (Santa Cruz, 1:200); rabbit
87   Peroxidase anti-Peroxidase (Sigma, 1:20000); rat anti-ribosomal protein S9 (1:1000); anti-
88   Trypanothione Reductase (rabbit, gift from L. Krauth-Siegel, BZH Heidelberg); Mouse anti-V5
89   (Biorad, 1:2000); anti-SCD6 and anti-DHH1 (from S. Kramer, University of Wurzburg, 1:10000
90   and 1:15000 respectively) and rabbit anti-BiP (from J. Bangs, University of Buffalo, 1:1000).

91   **Digitonin and stress granule fractionation**
92   For each sample, $3x10^7$ cells were collected by centrifugation at 2000 g for 10 min at 4°C. The
93   pellet was resuspended in 100 µl 1x PBS and centrifuged at 10000 g for 5 min at 4°C. The pellet
94   was then resuspended in 50 µl STE buffer (10 mM Tris-HCl pH 8.0, 150 mM NaCl, 1 mM EDTA)
95   and centrifuged at 10000 g for 5 min at 4°C. A 10 µg/µl digitonin stock solution was heated at
96   98°C for 5 min and cooled down before use. Seven different digitonin containing solutions, ranging
97   from 0-1.65 µg/µl digitonin, were prepared and each pellet was resuspended properly in 60 µl of
98   one solution. The samples were incubated at 25°C for 5 min and then centrifuged immediately at
99   10000 g and 4°C for 5 min. The supernatant was transferred to another tube containing 20 µl 4x
100   SDS-PAGE sample buffer. The pellet was washed twice with 1x PBS by centrifugation (4°C,
101   10000 g, 5 min) and finally resuspended in 80 µl 1x Laemmli buffer. Samples were analyzed by
102   Western Blotting. Stress granules were purified exactly as described in (Fritz et al. 2015), and
103   immunoprecipitations were done as described in (Singh et al. 2014).

104   **Immunofluorescence microscopy**
105   Tissue culture glass slides with 8 chambers were treated with 0.1% Poly-Lysine (Sigma, P-8920).
106   $2.5x10^6$ formaldehyde-fixed *T. brucei* were allowed to adhere to poly-lysine-treated chambered
107   slides (Falcon, 354108), permeabilised with 0.2% (w/v) Triton X-100 then incubated with protein-
108   specific antibodies followed fluorescently-labelled second antibodies in PBS containing 0.5%
109   gelatin. DNA was stained with 100 ng/ml DAPI (D9542, Sigma-Aldrich). Mitochondria were
110   detected by addition of Mitotracker Red CMXRos (50 nM, Thermo Fisher Scientific) to the cells 5
111   min prior to fixation. Images were examined using the Olympus IX81 microscope, 100x Oil
112   objective with a numerical aperture of 1.45. Digital images were taken with ORCA-R2 digital CCD
113   camera C10600 (Hamamatsu) and using the Xcellence RT software. The bright-field images were
114   taken using differential interference contrast (DIC). Fluorescent images were taken as Z-Stacks
115   with a height of roughly 4 µm and a step width of 0.2 µm. The images were deconvoluted (Wiener
116   Filter, Sub-Volume overlap: 20) and then processed using ImageJ. The background was
117   subtracted and brightness and contrast were adjusted automatically. The most in-focus image of
118   the deconvoluted stack was used.

119   **RNA preparation and Northern blotting**
120   $5x10^7$ cells were used for the extraction of total mRNA using peqGold Trifast (PeqLab). RNA was
121   separated on agarose-formaldehyde gels and blotted on a nylon membrane (Amersham Hybond-
122   N+, GE Healthcare, RPN203B). RNA was cross-linked on the membrane by UV light (0.2 J/cm^2)
123   and stained afterwards with methylene blue (SERVA) before hybridization with ^{32}P-labelled
124   probes, made using either the Prime-IT RmT Random Primer Labelling Kit (Stratagene) or, for
125   oligonucleotides, [γ^{32}P]ATP and T4 polynucleotide kinase (New England Biolabs).

126   **Affinity purification and mass spectrometry**
127   To purify TAP-ERBP1 for mass spectrometry, the protein was subjected to two steps of affinity
128   purification (Estévez et al. 2003). Briefly, the cleared lysate was incubated with IgG sepharose

129 beads, washed, and then bound proteins were released using TEV protease. The resulting
130 preparation was then allowed to adhere to a calmodulin affinity column, and proteins were eluted
131 with EGTA. Co-purifying proteins from three independent experiments were analyzed by LC/MS
132 by the ZMBH Mass Spectrometry facility. Cell lines expressing TAP-GFP served as control. Raw
133 data were analyzed using MaxQuant 1.5.8.3, with label-free quantification (LFQ), match between
134 runs (between triplicates), and the iBAQ algorithm enabled. The identified proteins were filtered
135 for known contaminants and reverse hits, as well as hits without unique peptides.

Affinity purification and RNASeq

137 For identification of associated RNAs (Droll et al. 2013), $1x10^9$ cells the cells were resuspended
138 in 50 ml ice-cold PBS, and UV-crosslinked (2 x 0.24 J/cm^2, Stratagene UV crosslinker) in two P15
139 Petri dishes on ice. They were then pelleted, snap-frozen and stored in liquid nitrogen before use.
140 The TAP-ERBP1 was allowed to bind to IgG beads, and the unbound lysate was retained as one
141 of the controls. The bound protein was released using TEV protease. Cross-linked proteins were
142 removed by proteinase K digestion (Droll et al. 2013) and RNA was extracted using peqGold
143 Trifast (peqLab) according to manufacturer's protocol. rRNA was depleted as required, by
144 incubation with complementary oligonucleotides and RNaseH (Minia et al. 2016). The NEBNext
145 Ultra RNA Library Prep Kit for Illumina (New England BioLab) was used for library preparation,
146 prior to sequencing with sequenced at EMBL (HiSeq 2000) to generate 50-base reads. Data were
147 analyzed using an in-house tool (10.5281/zenodo.165132) (Mulindwa et al. 2018).

148 **Results**

149 **ERBP1 is conserved in *Trypanosoma***
150 To investigate the function of ERBP1, we first analyzed its sequence. ERBP1 is a 55-kDa
151 protein with an isoelectric point of 5.73. It is predicted (by Phyre2) to consist predominantly of
152 alpha-helices. Homologues are found at the equivalent chromosomal position in other
153 *Trypanosoma* species, and in *Endotrypanum*, *Paratrypanosoma*, *Blechomonas* and *Bodo*, but
154 the gene appears to have been lost in *Leishmania*. The alignment (Supplementary Fig S1)
155 shows that the proteins share extremely acidic C-termini: for example, in *T. brucei*, the last 33
156 amino acid residues include 5 aspartates and 14 glutamates, as opposed to 3 lysines. Outside
157 the Kinetoplastida, the nearest matches were not with yeast Bfr1p, but with proteins of unknown
158 function in *Galdieria sulphuraria*, an acidiphilic red alga, and organisms from the SAR group that
159 probably have incorporated red algal endosymbionts: the oomycete *Phytophthora parasitica*, the
160 brown alga *Ectocarpus siliculosus* and the diatom *Phaeodactylum tricornutum*. The alignment
161 with all these proteins, as well as Bfr1p, showed little sequence identity between the
162 kinetoplastid sequences and all the others (S1 Fig).

164 **ERBP1 is required for normal growth but is not essential**
165 We first confirmed that ERBP1 is indeed required for normal growth of bloodstream-form
166 trypanosomes. To do this, we created bloodstream forms in which one *ERBP1* gene was modified
167 to encode a protein with an N-terminal V5 tag (V5-ERBP1). These were transfected with a
168 tetracycline-inducible construct for production of *ERBP1* dsRNA. Depletion of ERBP1 clearly
169 inhibited cell proliferation but the cells nevertheless survived (Fig 1).

170   Since some protein always remains after RNAi, we also tested the ability of the cells to survive in
171   the absence of the protein. Bloodstream form cells without ERBP1 (Fig 2A, B) also grew slower
172   than wild-type (Fig 2C), and this could be compensated by re-expression of the protein (Fig 2D).
173   Cells containing only a single tetracycline-inducible copy of ERBP1-myc (inducible on a knock-
174   out background, cKO) grew at similar rates to wild-type with or without tetracycline, but the protein
175   was clearly detectable in the absence of induction. The double band from ERBP1 was not always
176   seen but might be caused by acetylation (Moretti et al. 2018) or phosphorylation (Urbaniak et al.
177   2013). Despite these initial results, upon prolonged cultivation, the cells lacking ERBP1 gradually
178   increased their growth rate to wild-type. Survival and recovery of the cells after starvation was
179   also indistinguishable from wild-type (S2 Fig A). In procyclic forms, the endogenous ERBP1 gene
180   could be deleted only if an inducible ERBP1-myc gene was present. Depletion of the ERBP1-myc
181   had no effect on growth or recovery from starvation (S2 Fig B), but some residual ERBP1-myc
182   was doubtless present. It is, therefore, possible that ERBP1 is essential in procyclic forms, but
183   the failure of the deletion could also have been due to a technical problem.
184   The other high-throughput result that required verification was the effect of ERBP1 when tethered
185   to a reporter mRNA. Full-length ERBP1 had previously been identified as conferring a selective
186   advantage in the screen, suggesting that it could activate expression of the blasticidin resistance
187   marker. It gave no growth advantage in control cells in which the marker mRNA had no boxB
188   sequences, ruling out the possibility that ERBP1 expression by itself results in blasticidin
189   resistance. However, lambdaN-ERBP1 was unable to increase expression of a chloramphenicol
190   acetyltransferase reporter (S3 Fig). We have no explanation of this discrepancy: for both the
191   screen and the individual test, the lambdaN-myc sequence was placed at the N-terminus of the
192   open reading frame.

193   **ERBP1 is associated with the endoplasmic reticulum and with a second ER protein**
194   To examine the location of ERBP1 in bloodstream-form cells, we examined either N-terminally
195   V5-tagged ERBP1 (V5-ERBP1), or C-terminally myc-tagged ERBP1 (ERBP1-myc) expressed
196   from the endogenous locus (Fig 3 and 4). In both cases, ERBP1 clearly co-localized with the
197   endoplasmic reticulum and to some extent could be found in close proximity to mitochondria and
198   glycosome. We then conducted controlled-digitonin permeabilization studies to evaluate the
199   release of the protein with the same markers (Fig 5). ERBP1 was found to coelute partially with
200   the cytosolic marker but fully with the endoplasmic reticulum marker, suggesting that it is loosely
201   associated with the cytosolic face of the ER.
202   To investigate the interactions of ERBP1, we integrated a sequence encoding the tandem affinity
203   purification (TAP) tag into the genome such that the tag would be at the ERBP1 N-terminus (TAP-
204   ERBP1) while the other copy of *ERBP1* was deleted. TAP-tagged GFP served as the control.
205   Three proteins reproducibly co-purified with ERBP1: calmodulin, the ATP-dependent RNA
206   helicase HEL67/Vasa-like (Kramer et al. 2012), and a protein of unknown function encoded by
207   Tb927.9.9550 (S1 Table). Calmodulin quite often co-purifies with TAP-tagged proteins
208   (Schimanski et al. 2005). The association with the RNA helicase may be significant; although we
209   have detected it on many other mRNA-related purifications. Tb927.9.9550, however, was a novel
210   protein partner. It is conserved throughout Kinetoplastida, activated in the tethering screen (Erben
211   et al. 2014; Lueong et al. 2016), is in the mRNP proteome (Erben et al. 2014; Lueong et al. 2016),
212   but again lacks any recognizable domains; we, therefore, call it ERBP2. It appeared to be

213 essential in the high-throughput RNAi screen (Alsford et al. 2005), has a predicted signal peptide
214 and trans-membrane domain, and a GFP-tagged version, like ERBP1, localized to the ER in
215 procyclic form (Dean et al. 2016). To verify the interaction we used bloodstream-form cells
216 containing YFP-*in-situ* tagged ERBP1, with or without expression of ERBP2-myc. YFP-ERBP1
217 was pulled down with anti-myc antiserum only if ERBP2-myc was present, confirming the
218 interaction (Fig 6A), but the experiment also showed that - at least under the conditions used -
219 only a very small proportion of the ERBP1 was associated with ERBP2. This may, therefore, be
220 a transient interaction. ERBP2 is predicted to be predominantly alpha-helical, like ERBP1. The
221 isoelectric point of ERBP2 is 11, so it might interact with the highly acidic ERBP1 C-terminus.

222 **ERBP1 associates with mRNAs encoding ribosomal proteins, and not with starvation**
223 **stress granules**
224 Finally, we wished to know whether ERBP1 had any mRNA-binding specificity. We, therefore,
225 sequenced mRNAs that were co-purified with TAP-ERBP1 from bloodstream-form cells,
226 comparing them either with one unbound fraction or with the total mRNA. Unusually, the *ERBP1*
227 mRNA itself was not enriched, as would be expected from pull-down of the nascent polypeptide.
228 However, the two bound fractions clearly separated from all the controls (Fig 6B). Sixty four
229 mRNAs were enriched at least 2-fold in both pull-downs relative to all controls. Strikingly, nearly
230 half of them (29) encode ribosomal proteins. Two glycosomal membrane protein mRNAs, PMP4
231 and PEX11, were also enriched, but those encoding other PEX proteins - including other
232 glycosomal membrane proteins - were not, so the significance of this is uncertain. The length of
233 the associated mRNAs seemed to be important since both ribosomal and non-ribosomal targets
234 are shorter than the median (not shown).
235 It should be noted that the enrichment of mRNAs is calculated relative to the enrichment of other
236 mRNAs, and does not actually tell us which proportion of mRNAs with that sequence is associated
237 with the protein *in vivo.*
238 In budding yeast, Brf1 is associated with stress granules. To find out whether ERBP1 is stress-
239 granule associated, we incubated procyclic forms in PBS for 2 hours. Although clear granules
240 containing the marker SCD6 were formed (Fig 7A), V5-ERBP1 remained distributed throughout
241 the cytosol (Fig 7A) and was not associated with the granule fraction (Fig 7B). There is, therefore,
242 no evidence that ERBP1 is involved in the formation of stress granules or survival after starvation.

243 **Discussion**
244 Our results suggest that ERBP1 and its partner ERBP2 may modulate ribosomal expression, and
245 are both associated with the endoplasmic reticulum. Our results revealed both similarities and
246 differences between ERBP1 and Bfr1. Each is associated with the endoplasmic reticulum (Lang
247 et al. 2001), and each binds preferentially to mRNAs encoding ribosomal proteins (Lapointe et al.
248 2015). ERBP1, however, unlike Bfr1, does not show any preference for mRNAs encoding proteins
249 that are imported into the endoplasmic reticulum, and it does not associate with stress granules.
250 The latter observation is consistent with the exclusion of ribosomal protein mRNAs from
251 trypanosome stress granules (Fritz et al. 2015). ERBP1 is also associated with a kinetoplastid-
252 specific protein, ERBP2 which, like ERBP1, was detected in the mRNP proteome (Lueong et al.
253 2016).
254 Synthesis of ribosomes occupies considerable resources in all growing cells, which leads to a
255 requirement for coordination between ribosomal protein synthesis and rRNA transcription. In

256 mammalian cells and yeast, this coordination happens in the nucleus, at the level of transcription
257 (Albert et al. 2016; Calo et al. 2015). Trypanosomes also devote considerable resources to
258 ribosome synthesis: in bloodstream-forms, resources devoted to rRNA transcription are at least
259 as great as those needed for the synthesis of mRNAs (Haanstra et al. 2008), and the ribosomal
260 protein mRNAs together constitute more than 10% of total mRNA (Fadda et al. 2014). Feedback
261 inhibition of rRNA processing is known to occur in trypanosomes upon disruption of ribosome
262 assembly or export (Droll et al. 2010), but coordination of rRNA synthesis with ribosomal protein
263 availability - or vice-versa - has not been investigated. The mRNAs encoding trypanosome
264 ribosomal proteins are longer-lived than most others (Fadda et al. 2014), so at least in the short
265 term, control of their translation might be required in order to respond to altered conditions.
266 Ribosome densities on ribosomal protein mRNAs are significantly lower than on other mRNAs,
267 and most of the open reading frames are also relatively short (median 0.6 kb); consequently on
268 average there is only one ribosome per mRNA (Antwi et al. 2016). Low ribosome densities occur
269 if the rate of peptide chain elongation is fast relative to the rate of translation initiation. Ribosomal
270 protein mRNAs indeed have optimal codon usage (de Freitas Nascimento et al. 2018), which
271 would result in rapid elongation, and their short 5'-untranslated regions (Clayton 2019) might
272 assist scanning after 43S complex recruitment. These characteristics would lead to high
273 constitutive expression, but would also enable very rapid responses to altered conditions since,
274 at 5-10 residues per second, the single ribosome would run off in less than 1 minute. We,
275 therefore, suggest that several redundant pathways control ribosome protein synthesis, and one
276 of them includes ERBP1.
277

278 **Conclusions**
279 In *Trypanosoma brucei*, ribosomal protein encoding mRNAs seem to be excluded from starvation
280 stress granules; however, how granule exclusion of these mRNAs occurs is not known. Our
281 studies suggest that ERBP1 is an RNA-binding protein that associates with ribosomal mRNAs,
282 interacts with ERBP2, localizes to the cytosolic face of the endoplasmic reticulum and it does not
283 associate with stress granules. If ERBP1 is the trans-acting factor needed for the exclusion of
284 these mRNAs from starvation stress granules is still not known. As ERBP1 is required for normal
285 growth but is not essential, we suggest that redundant pathways control ribosome synthesis, and
286 one of them may include ERBP1.

287 **Acknowledgements**
288 We thank Nina Papavisiliou for generously hosting KB during the latter part of this project. We
289 also acknowledge Claudia Helbig and Ute Leibfried for technical support, David Ibberson of the
290 BioQuant sequencing facility for cDNA library construction, and the Mass spectrometry facility of
291 the ZMBH. We thank Luise Krauth-Siegel, (BZH Heidelberg), Susanne Kramer (University of
292 Würzberg) and Jay Bangs (University of Buffalo) for antibodies, and Pia Hartwig for work done
293 during a lab rotation.

294 **References**
295

296 Albert B, Knight B, Merwin J, Martin V, Ottoz D, Gloor Y, Bruzzone MJ, Rudner A, and Shore D.
297   2016. A Molecular Titration System Coordinates Ribosomal Protein Gene Transcription
298   with Ribosomal RNA Synthesis. *Mol Cell* 64:720-733. 10.1016/j.molcel.2016.10.003
299 Alibu VP, Storm L, Haile S, Clayton C, and Horn D. 2004. A doubly inducible system for RNA
300   interference and rapid RNAi plasmid construction in *Trypanosoma brucei*. *Mol Biochem
301   Parasitol* 139:75-82.
302 Alsford S, Glover L, and Horn D. 2005. Multiplex analysis of RNA interference defects in
303   Trypanosoma brucei. *Mol Biochem Parasitol* 139:129-132.
304 Antwi E, Haanstra J, Ramasamy G, Jensen B, Droll D, Rojas F, Minia I, Terrao M, Mercé C,
305   Matthews K, Myler P, Parsons M, and Clayton C. 2016. Integrative analysis of the
306   *Trypanosoma brucei* gene expression cascade predicts differential regulation of mRNA
307   processing and unusual control of ribosomal protein expression. *BMC Genomics* 17:306.
308   10.1186/s12864-016-2624-3
309 Beckmann BM, Horos R, Fischer B, Castello A, Eichelbaum K, Alleaume AM, Schwarzl T, Curk
310   T, Foehr S, Huber W, Krijgsveld J, and Hentze MW. 2015. The RNA-binding proteomes
311   from yeast to man harbour conserved enigmRBPs. *Nat Commun* 6:10127.
312 Calo E, Flynn RA, Martin L, Spitale RC, Chang HY, and Wysocka J. 2015. RNA helicase
313   DDX21 coordinates transcription and ribosomal RNA processing. *Nature* 518:249-253.
314   10.1038/nature13923
315 Clayton C. 2019. Control of gene expression in trypanosomatids: living with polycistronic
316   transcription. *Royal Society Open Biology* 9:190072. 10.1098/rsob.190072
317 Clayton CE. 1987. Import of fructose bisphosphate aldolase into the glycosomes of
318   *Trypanosoma brucei*. *J Cell Biol* 105:2649-2653.
319 de Freitas Nascimento J, Kelly S, Sunter J, and Carrington M. 2018. Codon choice directs
320   constitutive mRNA levels in trypanosomes. *Elife* 7. 10.7554/eLife.32467
321 Dean S, Sunter J, and Wheeler R. 2016. TrypTag.org: A trypanosome genome-wide protein
322   localisation resource. *Trends Parasitol* 33:80-82.
323 Droll D, Archer S, Fenn K, Delhi P, Matthews K, and Clayton C. 2010. The trypanosome
324   Pumilio-domain protein PUF7 associates with a nuclear cyclophilin and is involved in
325   ribosomal RNA maturation. *FEBS Lett* 84:1156-1162. 10.1016/j.febslet.2010.02.018
326 Droll D, Minia I, Fadda A, Singh A, Stewart M, Queiroz R, and Clayton C. 2013. Post-
327   transcriptional regulation of the trypanosome heat shock response by a zinc finger
328   protein. *PLoS Pathog* 9:e1003286.
329 Erben E, Fadda A, Lueong S, Hoheisel J, and Clayton C. 2014. Genome-wide discovery of
330   post-transcriptional regulators in *Trypanosoma brucei*. *PLoS Pathog* 10:e1004178.
331   doi:10.1371/journal.ppat.1004178
332 Estévez AM, Lehner B, Sanderson CM, Ruppert T, and Clayton C. 2003. The roles of inter-
333   subunit interactions in exosome stability. *J Biol Chem* 278:34943-34951.
334 Fadda A, Ryten M, Droll D, Rojas F, Färber V, Haanstra J, Bakker B, Matthews K, and Clayton
335   C. 2014. Transcriptome-wide analysis of mRNA decay reveals complex degradation
336   kinetics and suggests a role for co-transcriptional degradation in determining mRNA
337   levels. *Mol Microbiol* 94:307-326. 10.1111/mmi.12764
338 Fritz M, Vanselow J, Sauer N, Lamer S, Goos C, Siegel T, Subota I, Schlosser A, Carrington M,
339   and Kramer S. 2015. Novel insights into RNP granules by employing the trypanosome's
340   microtubule skeleton as a molecular sieve. *Nucleic Acids Res* 43:8013-8032.
341 Haanstra J, Stewart M, Luu V-D, van Tuijl A, Westerhoff H, Clayton C, and Bakker B. 2008.
342   Control and regulation of gene expression: quantitative analysis of the expression of
343   phosphoglycerate kinase in bloodstream form *Trypanosoma brucei*. *J Biol Chem*
344   283:2495-2507.
345 Hentze MW, Castello A, Schwarzl T, and Preiss T. 2018. A brave new world of RNA-binding
346   proteins. *Nat Rev Mol Cell Biol*. 10.1038/nrm.2017.130

347   Jackson CL, and Kepes F. 1994. BFR1, a multicopy suppressor of brefeldin A-induced lethality,
348   is implicated in secretion and nuclear segregation in Saccharomyces cerevisiae.
349   *Genetics* 137:423-437.
350   Jeacock L, Faria J, and Horn D. 2018. Codon usage bias controls mRNA and protein
351   abundance in trypanosomatids. *Elife* 7. 10.7554/eLife.32496
352   Kramer S, Marnef A, Standart N, and Carrington M. 2012. Inhibition of mRNA maturation in
353   trypanosomes causes the formation of novel foci at the nuclear periphery containing
354   cytoplasmic regulators of mRNA fate. *J Cell Sci* 125:2896-2909. 10.1242/jcs.099275
355   Lang BD, Li A, Black-Brewster HD, and Fridovich-Keil JL. 2001. The brefeldin A resistance
356   protein Bfr1p is a component of polyribosome-associated mRNP complexes in yeast.
357   *Nucleic Acids Res* 29:2567-2574. 10.1093/nar/29.12.2567
358   Lapointe CP, Wilinski D, Saunders HA, and Wickens M. 2015. Protein-RNA networks revealed
359   through covalent RNA marks. *Nat Methods* 12:1163-1170. 10.1038/nmeth.3651
360   Low YS, Bircham PW, Maass DR, and Atkinson PH. 2014. Kinetochore genes are required to
361   fully activate secretory pathway expansion in S. cerevisiae under induced ER stress. *Mol*
362   *Biosyst* 10:1790-1802. 10.1039/c3mb70414a
363   Lueong S, Merce C, Fischer B, Hoheisel J, and Erben E. 2016. Gene expression regulatory
364   networks in *Trypanosoma brucei*: insights into the role of the mRNA-binding proteome.
365   *Mol Microbiol* 100:457-471.
366   Minia I, Merce C, Terrao M, and Clayton C. 2016. Translation regulation and RNA granule
367   formation after heat shock of procyclic form *Trypanosoma brucei*: many heat-induced
368   mRNAs are increased during differentiation to mammalian-infective forms. *PLoS Negl*
369   *Trop Dis* 10:e0004982.
370   Moretti NS, Cestari I, Anupama A, Stuart K, and Schenkman S. 2018. Comparative Proteomic
371   Analysis of Lysine Acetylation in Trypanosomes. *J Proteome Res* 17:374-385.
372   10.1021/acs.jproteome.7b00603
373   Mulindwa J, Leiss K, Ibberson D, Kamanyi Marucha K, Helbig C, Melo do Nascimento L,
374   Silvester E, Matthews K, Matovu E, Enyaru J, and Clayton C. 2018. Transcriptomes of
375   *Trypanosoma brucei rhodesiense* from sleeping sickness patients, rodents and culture:
376   Effects of strain, growth conditions and RNA preparation methods. *PLoS Negl Trop Dis*
377   12:e0006280. 10.1371/journal.pntd.0006280
378   Schimanski B, Nguyen T, and Günzl A. 2005. Highly efficient tandem affinity purification of
379   trypanosome protein complexes based on a novel epitope combination. *Eukaryot Cell*
380   4:1942-1950.
381   Simpson CE, Lui J, Kershaw CJ, Sims PF, and Ashe MP. 2014. mRNA localization to P-bodies
382   in yeast is bi-phasic with many mRNAs captured in a late Bfr1p-dependent wave. *J Cell*
383   *Sci* 127:1254-1262. 10.1242/jcs.139055
384   Singh A, Minia I, Droll D, Fadda A, Clayton C, and Erben E. 2014. Trypanosome MKT1 and the
385   RNA-binding protein ZC3H11: interactions and potential roles in post-transcriptional
386   regulatory networks. *Nucleic Acids Res* 42:4652-4668. 10.1093/nar/gkt1416
387   Urbaniak MD, Martin D, and Ferguson MA. 2013. Global quantitative SILAC phosphoproteomics
388   reveals differential phosphorylation is widespread between the procyclic and
389   bloodstream form lifecycle stages of *Trypanosoma brucei*. *J Proteome Res* 12:2233-
390   2244. 10.1021/pr400086y
391   Weidner J, Wang C, Prescianotto-Baschong C, Estrada AF, and Spang A. 2014. The polysome-
392   associated proteins Scp160 and Bfr1 prevent P body formation under normal growth
393   conditions. *J Cell Sci* 127:1992-2004. 10.1242/jcs.142083
394   Xue Z, Shan X, Sinelnikov A, and Melese T. 1996. Yeast mutants that produce a novel type of
395   ascus containing asci instead of spores. *Genetics* 144:979-989.
396

Figure 1

ERBP1 is required for normal growth of bloodstream-form *T. brucei.*

Bloodstream forms in which one *ERBP1* gene was V5-tagged *in situ* at the 5'-end were used, with inducible expression of stem-loop *ERBP1* dsRNA. **A.** Depletion of V5-ERBP1 after RNAi.

3×10^6 cells were collected each day and V5-ERBP1 was detected by Western Blotting. Aldolase was used as loading control. Numbers below the blot indicate the quantification of the V5-ERBP1 signals normalized to the uninduced RNAi at day 0. **B.** Growth curve for three Tet+ (red) and Tet- (grey) clones analysed in three independent experiments. **C**. Doubling times (in h) for the 3 experiments are shown.
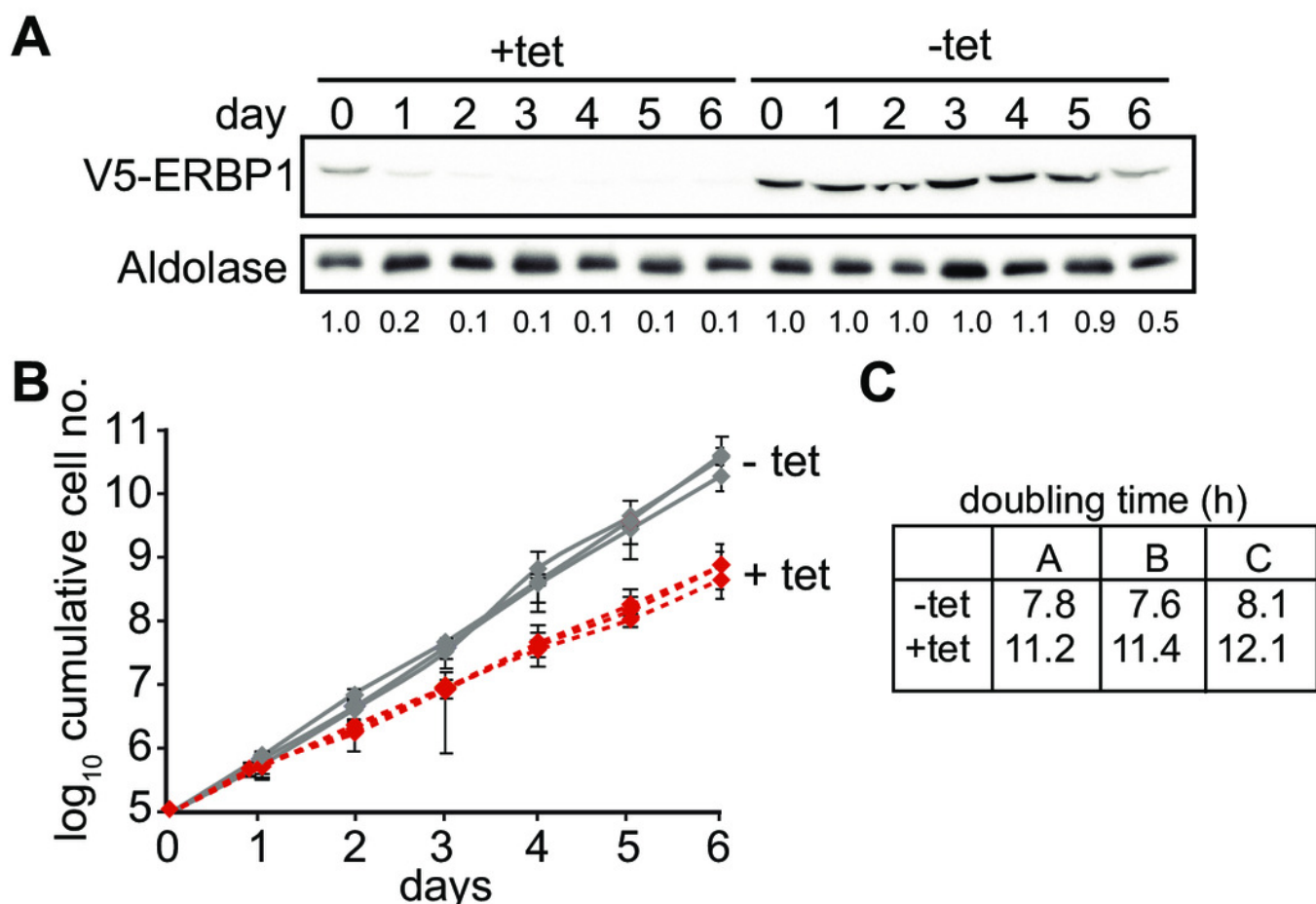
Figure 2

Bloodstream-form trypanosomes survive without ERBP1.

A. Schematic representation of the *ERBP1* gene before and after replacement with selectable marker genes. Primers for PCR and corresponding product lengths (in kb) are shown. **B**. DNA from wild type (wt) and double knock-out (dKO) cells was analysed by PCR using the primers shown in (A). The primers used are indicated above each image. **C**. Cumulative growth curve for 3 independent experiments, each with three different clones for wild-type (wt), single knock-out (sKO) and double knock-out (dKO). Error bars indicate standard deviation from results for 3 clones; each was measured 3 times then for each, and average was taken. **D**. Expression of ERBP1-myc complements the defect in dKO cells. The dKO cells were complemented with tetracycline-inducible ERBP1-myc (complemented KO; cKO). The graph shows the cumulative parasite numbers. **E**. Western blot from (D) using 3×10^6 cells/lane. Some ERBP1-myc is detectable in the absence of tetracycline inducer. **F**. As (D) but for procyclic forms. As homozygous gene replacement failed in procyclic forms, the sKO cells were complemented with tetracycline-inducible ERBP1-myc. **G**. Western blot from (F) using 3×10^6 cells/lane. Aldolase was used as loading control.
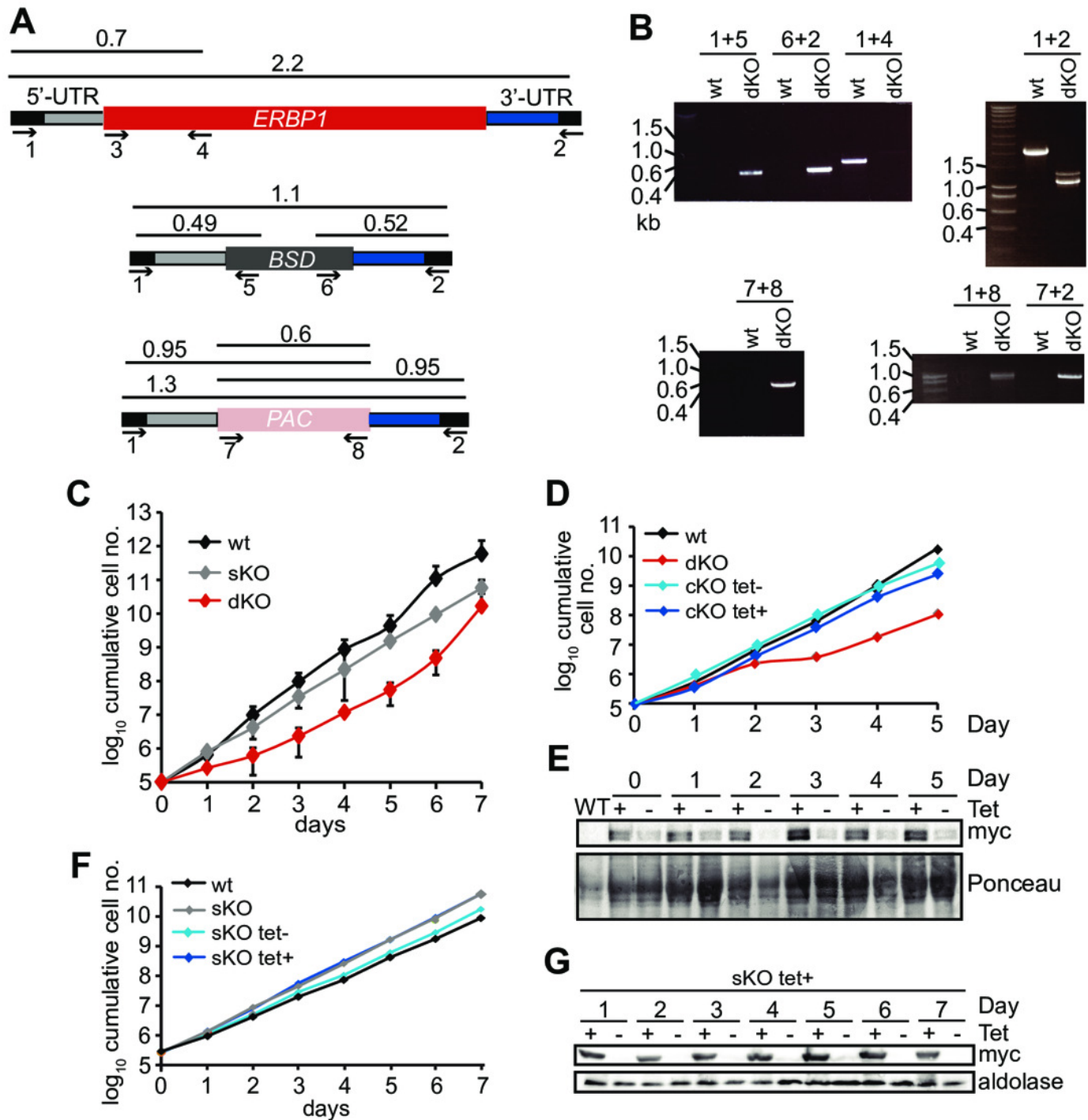
Figure 3

V5-ERBP1 colocalises with the endoplasmic reticulum.

Bloodstream forms expressing N-terminally V5-tagged ERBP from the endogenous locus (V5-ERBP1) were examined by immunofluorescence microscopy. Cells without V5 served as control. Nuclear and kinetoplast DNA was stained with DAPI (blue). Representative images are shown for three independent experiments. Z-stacks were examined using the Olympus CellR microscope and 100 x magnification, and Images were deconvoluted. Scale bar: 10 µm. **A.** V5-ERBP1 is red and cytosolic Trypanothione Reductase (=TR) is green. **B.** V5-ERBP1 is red and glycosomal aldolase is green. **C.** V5-ERBP1 is green and mitotracker is red **D.** V5-ERBP1 is red and the endoplasmic reticulum marker BiP is green.
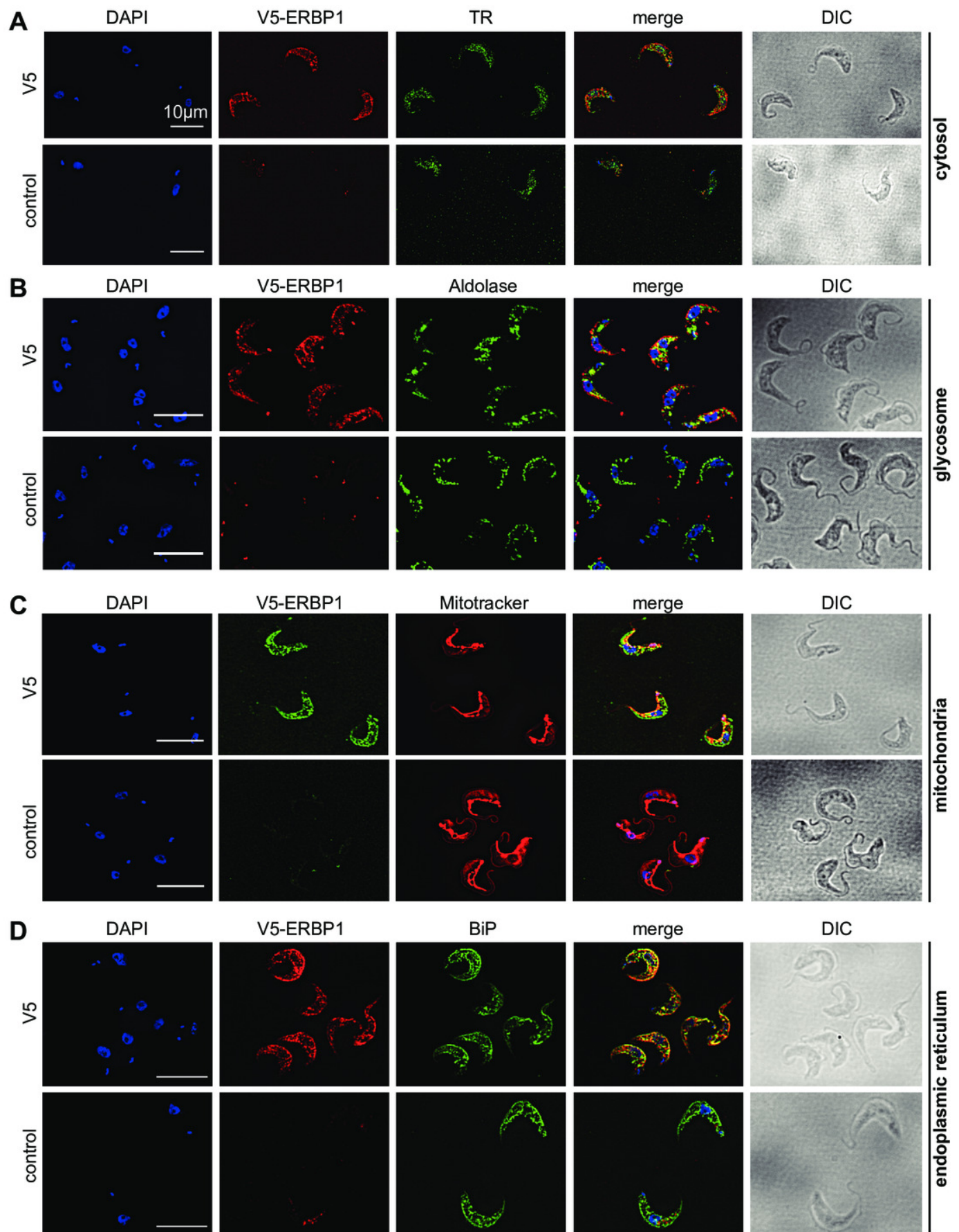
Figure 4

ERBP1-myc colocalises with the endoplasmic reticulum.

Bloodstream forms expressing C-terminally myc-tagged ERBP from the endogenous locus (ERBP1-myc) were examined by immunofluorescence microscopy. Cells without myc served as control. Nuclear and kinetoplast DNA was stained with DAPI (blue). Representative images are shown for three independent experiments. Z-stacks were examined using the Olympus CellR microscope and 100 x magnification, and Images were deconvoluted. Scale bar: 10 µm. **A.** ERBP1-myc is red and cytosolic Trypanothione Reductase (TR) is green. **B.** ERBP1-myc is red and glycosomal aldolase is green. **C.** ERBP1-myc is green and mitotracker is red **D.** ERBP1-myc is red and the endoplasmic reticulum marker BiP is green.

A

DAPI	ERBP1-myc	TR	merge	DIC

myc

control

cytosol

B

DAPI	ERBP1-myc	Aldolase	merge	DIC

myc

control

glycosome

C

DAPI	ERBP1-myc	Mitotracker	merge	DIC

myc

control

mitochondria

D

DAPI	ERBP1-myc	BiP	merge	DIC

myc

control

endoplasmic reticulum
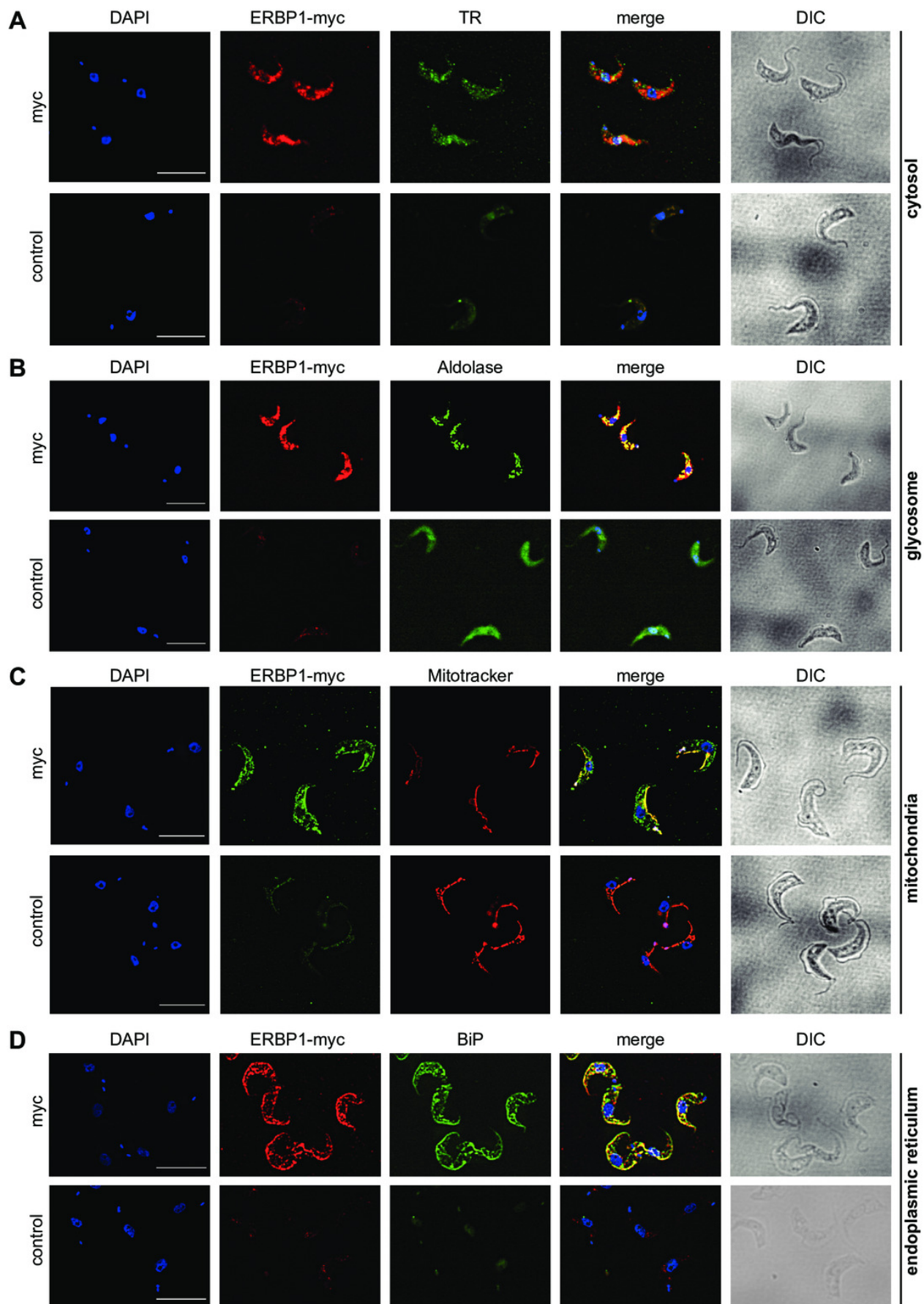
Figure 5

ERBP1 is not inside a membrane-bound compartment.

Bloodstream-form cells expressing V5-ERBP1 (**A**) or ERBP1-myc (**B**) were treated with increasing digitonin:protein (mg:mg) ratios as indicated at the top. Samples were centrifuged and the supernatant and pellet were analysed by Western Blotting. Numbers below the blots indicate quantification of the corresponding signal. Aldolase (glycosome); TR: Trypanothione Reductase (cytosol); LipDH: Lipoamide Dehydrogenase (mitochondria); BiP: Binding Immunoglobulin Protein (ER).
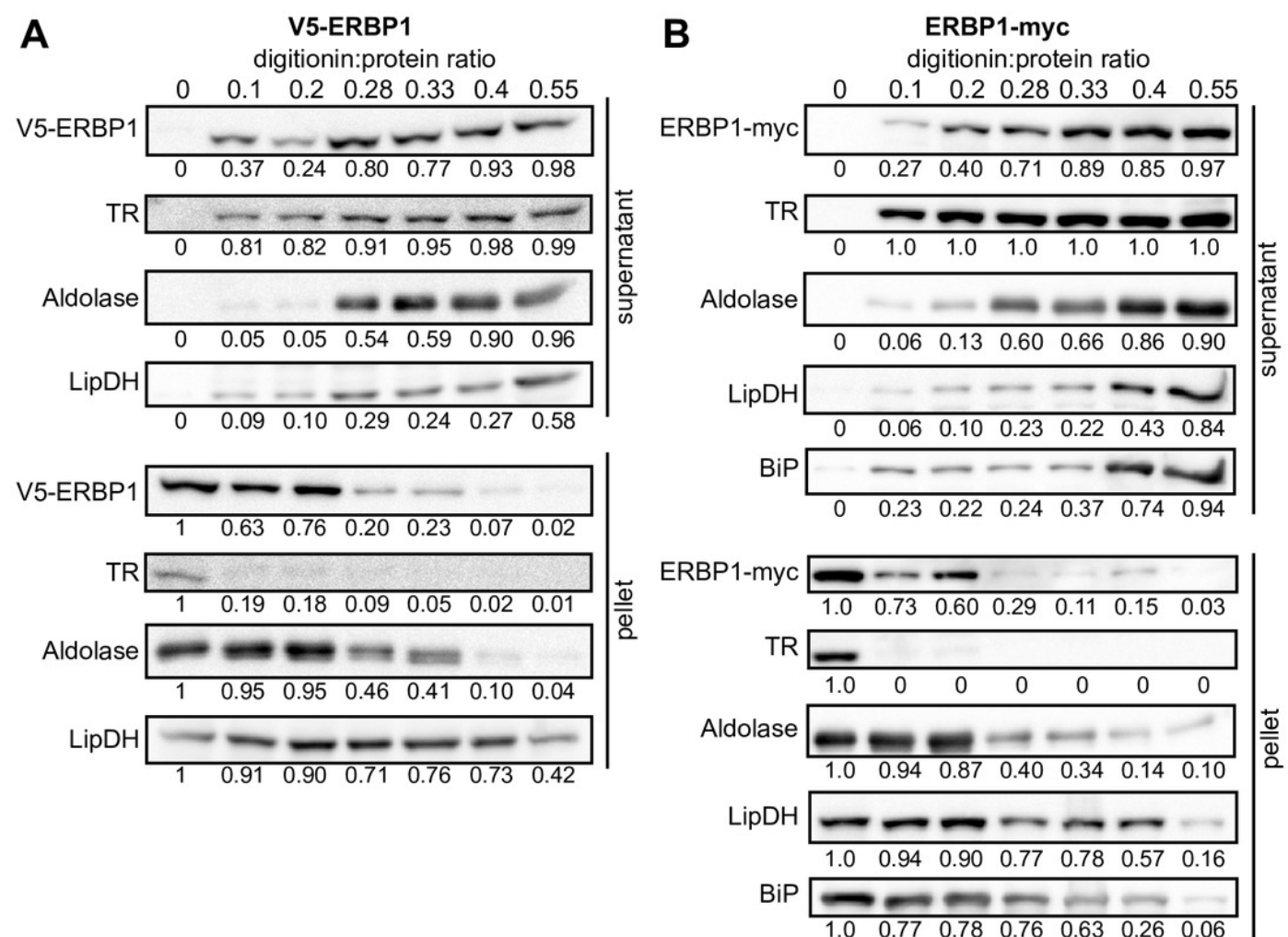
Figure 6

Interactions of ERBP1.

A. ERBP2 co-precipitates with ERBP1. Extracts were made from cells expressing YFP-ERBP1, with or without ERBP2-myc. After immunoprecipitation with anti-myc, a Western blot was probed for myc and for YFP as indicated. The stained membrane is shown below. I = input; UB = unbound fraction; E = eluate from anti-myc immunoprecipitation. **B.** Principal component analysis of transcriptomes after RNA-Seq of total mRNA (WT) and after pull-down of TAP-ERBP1; UB = unbound; B = bound (eluate from the affinity matrix). **C.** Functions of proteins encoded by ERBP1-associated mRNAs. The pie chart show the distributions for mRNAs that were at least 2-fold enriched in both bound fractions relative to the controls. Details are in supplementary Table S2.

A

B

C
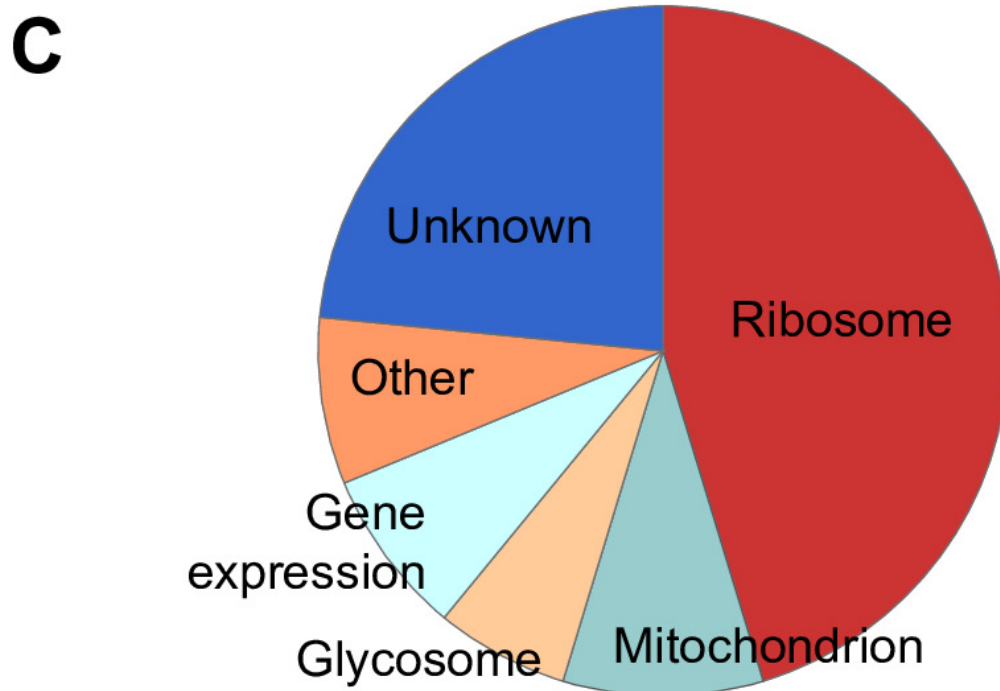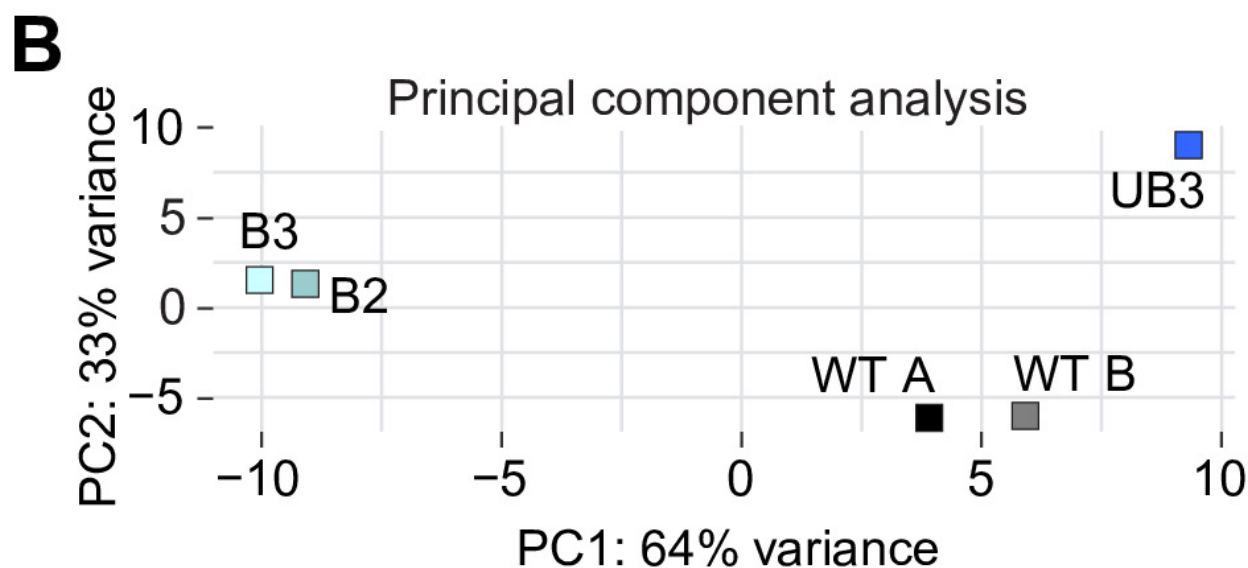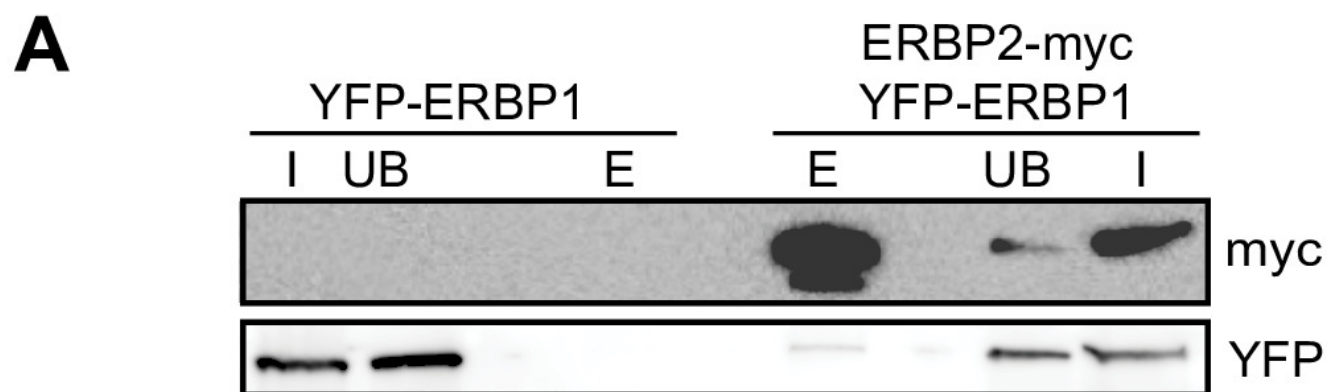
Figure 7

V5-ERBP1 is not concentrated in starvation stress granules.

A. Procyclic forms expressing V5-ERBP1 were incubated for 2h in 1xPBS, then fixed and stained for V5 (red) and the stress granule marker SCD6 (green). Nuclear and kinetoplast DNA were stained with DAPI (blue). Z-stacks were examined using the Olympus CellR microscope and 100 x magnification. Images were deconvoluted. The control was not starved in PBS. **B.** V5-ERBP1-expressing procyclic forms were starved as in (A) and then fractionated to concentrate stress granules.